

Geometrical spreading of P-waves in horizontally layered, azimuthally anisotropic media

Xiaoxia Xu¹, Ilya Tsvankin¹, and Andrés Pech²

ABSTRACT

For processing and inverting reflection data, it is convenient to represent geometrical spreading through the reflection traveltimes measured at the earth's surface. Such expressions are particularly important for azimuthally anisotropic models in which variations of geometrical spreading with both offset and azimuth can significantly distort the results of wide-azimuth amplitude-variation-with-offset (AVO) analysis.

Here, we present an equation for relative geometrical spreading in laterally homogeneous, arbitrarily anisotropic media as a simple function of the spatial derivatives of reflection traveltimes. By employing the Tsvankin-Thomsen nonhyperbolic moveout equation, the spreading is represented through the moveout coefficients, which can be estimated from surface seismic data. This formulation is then applied to P-wave reflections in an orthorhombic layer to evaluate the distortions of the geometrical spreading caused by both polar and azimuthal anisotropy.

The relative geometrical spreading of P-waves in homogeneous orthorhombic media is controlled by five parameters that are also responsible for time processing. The weak-anisotropy approximation, verified by numerical tests, shows that azimuthal velocity variations contribute significantly to geometrical spreading, and the existing equations for transversely isotropic media with a vertical symmetry axis (VTI) cannot be applied even in the vertical symmetry planes. The shape of the azimuthally varying spreading factor is close to an ellipse for offsets smaller than the reflector depth but becomes more complicated for larger offset-to-depth ratios. The overall magnitude of the azimuthal variation of the geometrical spreading for the moderately anisotropic model used in the tests exceeds 25% for a wide range of offsets.

While the methodology developed here is helpful in modeling and analyzing anisotropic geometrical spreading, its main practical application is in correcting the wide-azimuth AVO signature for the influence of the anisotropic overburden.

INTRODUCTION

Inversion of prestack amplitude variation with offset and azimuth (azimuthal AVO analysis) represents one of the most effective tools for characterizing naturally fractured reservoirs. The presence of preferentially oriented fractures or horizontal stresses makes the reservoir formation azimuthally anisotropic, and wide-azimuth reflection amplitudes can be used to estimate fracture orientation and, in some cases, to map the lateral variation of the fracture density (Mallick et al., 1998; Lynn et al., 1999; Bakulin et al., 2000; Rüger, 2001). The main advantage of amplitude methods compared to traveltimes inversion is their high vertical resolution, which makes AVO analysis applicable to relatively thin reservoir layers.

The amplitude signature of reflected waves is controlled by the radiation pattern of the source, geometrical spreading, attenuation, the reflection/transmission coefficients along the raypath, and the conversion coefficients at the receiver (Martinez, 1993; Maultzsch et al., 2003). Since AVO analysis operates with the reflection coefficient at the target horizon, an essential element of AVO processing is removal of the influence of all other factors from the measured amplitude. If the medium is not strongly attenuative, geometrical spreading typically makes the most significant contribution to the amplitude distortion above the target horizon (Martinez, 1993; Ursin and Hokstad, 2003). In particular, if the overburden is anisotropic (e.g., shales in a sand-shale sequence), it acts as a 3D focusing lens that may significantly change the

Manuscript received by the Editor January 15, 2004; revised manuscript received February 15, 2005; published online September 8, 2005.

¹Colorado School of Mines, Center for Wave Phenomena, Department of Geophysics, Golden, Colorado 80401-1887. E-mail: xiaoxia@dix.mines.edu; ilya@dix.mines.edu.

²Formerly Colorado School of Mines, Center for Wave Phenomena, Department of Geophysics, Golden, Colorado; presently Instituto Politécnico Nacional, CIIDIR-Unidad Oaxaca, Calle Hornos 1003, Santa Cruz Xoxocotlan, Oaxaca, Mexico. E-mail: apech@ipn.mx.

© 2005 Society of Exploration Geophysicists. All rights reserved.

amplitude distribution along the wavefront of the reflected wave (Tsvankin, 1995, 2001). Therefore, estimation of the reflection coefficient for targets beneath anisotropic layers may be strongly distorted without an accurate geometrical-spreading correction.

The most straightforward way to compute anisotropic geometrical spreading is by performing dynamic ray tracing (Gajewski and Pšenčík, 1990). For simple homogeneous models, it is possible to use analytic approximations of the Green's function, such as those presented by Tsvankin (1995, 2001) for P- and SV-waves in a transversely isotropic (TI) layer. Modeling methods, however, require accurate information about the anisotropic velocity field for the whole overburden, which is seldom available in practice.

An alternative approach, more suitable for AVO processing, is based on relating geometrical spreading to the traveltimes of reflection events recorded at the surface. For example, Vanelle and Gajewski (2003) present an algorithm to determine geometrical spreading from coarsely gridded traveltimes tables. Ursin and Hokstad (2003) express geometrical spreading in stratified transversely isotropic media with a vertical symmetry axis (VTI) in terms of the reflection traveltimes and the group angle in the subsurface layer. For horizontally layered VTI models, P-wave traveltimes can be described accurately by a nonhyperbolic moveout equation parameterized by just two moveout coefficients: the effective NMO velocity V_{nmo} and the effective anellipticity parameter η (Alkhalifah and Tsvankin, 1995). The best-fit parameters V_{nmo} and η can be estimated, for example, by a 2D semblance scan (Grechka and Tsvankin, 1998), which makes it possible to compute geometrical spreading using surface reflection data solely (Ursin and Hokstad, 2003). This approach can also be used to find analytic expressions for geometrical spreading in VTI media in terms of the parameters V_{nmo} and η .

The distortions caused by geometrical spreading in reflection amplitudes are even more pronounced for azimuthally anisotropic media (Rüger and Tsvankin, 1997; Maultzsch et al., 2003). Here, we use ray theory to obtain a simple traveltimes-based equation for the geometrical spreading of pure (unconverted) reflected waves recorded over horizontally layered arbitrarily anisotropic media. By combining this result with the Tsvankin-Thomsen moveout equation for an orthorhombic layer with a horizontal symmetry plane, we express the spreading as a function of the azimuthally varying moveout coefficients. Application of the weak-anisotropy approximation helps to explain the dependence of relative geometrical spreading on the anisotropic parameters of orthorhombic media both within and outside the vertical symmetry planes. Numerical tests verify the accuracy of the analytic results and illustrate the character of the amplitude distortions caused by the azimuthally varying geometrical spreading.

RELATIVE GEOMETRICAL SPREADING AS A FUNCTION OF REFLECTION TRAVELTIME

Geometrical spreading describes the amplitude decay of an elastic wave caused by the expansion of its wavefront away from the source. The relative geometrical spreading $L(R, S)$ between the source S and the receiver R is an essential part of the ray-theory Green's function G_{in} (Červený, 2001, equation

5.4.24):

$$G_{in}(R, t; S, t_0) = \frac{g_n(S)g_i(R) \exp[iT^G(R, S)]}{4\pi[\rho(S)\rho(R)V(S)V(R)]^{1/2}L(R, S)} \times R^C \delta[t - t_0 - T(R, S)], \quad (1)$$

where t and t_0 are the recording and excitation times, respectively; $\rho(S)$ and $V(S)$ are density and phase velocity at the source; $\rho(R)$ and $V(R)$ are the same quantities at the receiver; $g_n(S)$ and $g_i(R)$ are the polarization vectors at the source and receiver; $T^G(R, S)$ is the complete phase shift; R^C is the product of the reflection/transmission coefficients normalized with respect to the vertical energy flux at all interfaces crossed by the ray; $\delta(t)$ is the delta function; and $T(R, S)$ is the traveltimes.

Throughout this paper, we address relative geometrical spreading $L(R, S)$ defined by equation 4.10.11 in Červený (2001). The factor $L(R, S)$ can be expressed through the spatial derivatives of the traveltimes T around a raypath (Červený, 2001, equation 4.10.50; Goldin, 1986):

$$L(R, S) = \sqrt{\frac{\cos \phi^s \cos \phi^r}{|\det \mathbf{M}^{\text{mix}}(R, S)|}}, \quad (2)$$

where ϕ^s is the angle between the ray and the normal to the surface at the source, ϕ^r is the ray angle at the receiver, and the matrix \mathbf{M}^{mix} is given by (Červený, 2001, equation 4.10.46)

$$\mathbf{M}^{\text{mix}} = \begin{bmatrix} \frac{\partial^2 T(x^r, x^s)}{\partial x_1^s \partial x_1^r} & \frac{\partial^2 T(x^r, x^s)}{\partial x_1^s \partial x_2^r} \\ \frac{\partial^2 T(x^r, x^s)}{\partial x_2^s \partial x_1^r} & \frac{\partial^2 T(x^r, x^s)}{\partial x_2^s \partial x_2^r} \end{bmatrix}; \quad (3)$$

(x_1^s, x_2^s) and (x_1^r, x_2^r) are the local Cartesian coordinates of the source and receiver.

For a reflected wave recorded at a horizontal surface, equation 2 can be reduced to the following function of the traveltimes T (see Appendix A):

$$L(R, S) = L(x, \alpha) = (\cos \phi^s \cos \phi^r)^{1/2} \times \left[\frac{\partial^2 T}{\partial x^2} \frac{\partial T}{\partial x} \frac{1}{x} + \frac{\partial^2 T}{\partial x^2} \frac{\partial^2 T}{\partial \alpha^2} \frac{1}{x^2} - \left(\frac{\partial T}{\partial \alpha} \right)^2 \frac{1}{x^4} \right]^{-1/2}, \quad (4)$$

where x is the source-receiver offset and α is the azimuth of the source-receiver line. Equation 4 is valid for pure (unconverted) modes in laterally homogeneous (but possible vertically heterogeneous) media, regardless of the anisotropic symmetry.

In addition to providing a concise representation of the spreading $L(R, S)$ factor in terms of the reflection traveltimes $T(x, \alpha)$, equation 4 helps to gain insight into the influence of both polar and azimuthal velocity variations on geometrical spreading. The first term in the brackets coincides with the geometrical-spreading factor for horizontally layered VTI media (Ursin and Hokstad, 2003), where the traveltimes T is independent of the azimuth α . Note, however, that even this term is distorted by azimuthal anisotropy because the traveltimes derivatives with respect to offset vary with α . The second and third terms appear only in azimuthally anisotropic media.

GEOMETRICAL SPREADING IN HOMOGENEOUS ORTHORHOMBIC MEDIA

Effective orthorhombic models resulting from one or two fracture sets are considered typical for naturally fractured reservoirs (Schoenberg and Helbig, 1997; Bakulin et al., 2000). Here, we apply the general expression 4 to reflections from the bottom of a single horizontal orthorhombic layer with a horizontal symmetry plane (Figure 1). The incidence and reflection group angles for this model are equal to each other (i.e., $\phi^s = \phi^r = \phi$), and equation 4 becomes

$$L(x, \alpha) = \cos \phi \left[\frac{\partial^2 T}{\partial x^2} \frac{\partial T}{\partial x} \frac{1}{x} + \frac{\partial^2 T}{\partial x^2} \frac{\partial^2 T}{\partial \alpha^2} \frac{1}{x^2} - \left(\frac{\partial T}{\partial \alpha} \right)^2 \frac{1}{x^4} \right]^{-1/2} \quad (5)$$

Orthorhombic media with a horizontal symmetry plane have two mutually orthogonal vertical symmetry planes, in which the first derivative $\partial T/\partial \alpha$ goes to zero and equation 5 further simplifies to

$$L(x) = \cos \phi \left[\frac{\partial^2 T}{\partial x^2} \frac{\partial T}{\partial x} \frac{1}{x} + \frac{\partial^2 T}{\partial x^2} \frac{\partial^2 T}{\partial \alpha^2} \frac{1}{x^2} \right]^{-1/2} \quad (6)$$

Equation 6 confirms the conclusion of Tsvankin (1997, 2001) that the kinematic equivalence between the symmetry planes of orthorhombic and VTI media cannot be extended to geometrical spreading. The second derivative, $\partial^2 T/\partial \alpha^2$, which generally does not vanish in the symmetry planes, reflects the influence of azimuthal velocity variations on symmetry-plane amplitudes. This 3D character of geometrical spreading in the symmetry planes is explained by the dependence of the wavefront curvature on both in-plane and out-of-plane (azimuthal) velocity variations. The spreading $L(x, \alpha)$ for source-receiver lines outside the symmetry planes (equation 5) also depends on the first derivative, $\partial T/\partial \alpha$.

Nonhyperbolic moveout equation for an orthorhombic layer

Reflection moveout, as well as other signatures of reflected waves in orthorhombic media, is conveniently described using the notation suggested by Tsvankin (1997, 2001). Tsvankin's parameter definitions are based on the analogous form of the Christoffel equation in the symmetry planes of orthorhombic

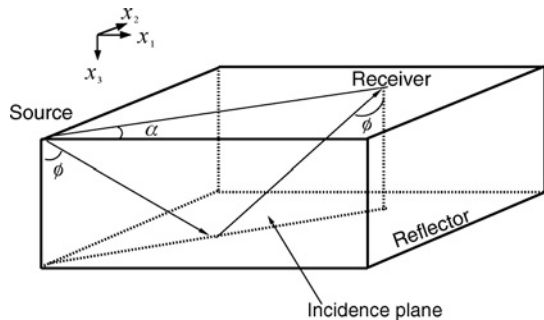


Figure 1. Reflected ray in a homogeneous horizontal orthorhombic layer with a horizontal symmetry plane. The ray lies in the incidence plane, although the corresponding phase-velocity vector may point out of plane.

(Figure 2) and VTI media. The anisotropic parameters $\epsilon^{(1)}$, $\delta^{(1)}$, and $\gamma^{(1)}$ play the roles of Thomsen's (1986) VTI coefficients ϵ , δ , and γ in the vertical symmetry plane $[x_2, x_3]$ (the superscript denotes the orthogonal axis x_1). The similar set of anisotropic coefficients in the $[x_1, x_3]$ plane includes $\epsilon^{(2)}$, $\delta^{(2)}$, and $\gamma^{(2)}$. One more anisotropic coefficient, $\delta^{(3)}$, is defined in the horizontal plane $[x_1, x_2]$. The parameter V_{P0} denotes the vertical P-wave velocity, and V_{S0} is the velocity of the vertically propagating S-wave polarized in the x_1 -direction.

Although orthorhombic symmetry is described by nine independent parameters (for a fixed orientation of the symmetry planes), kinematic signatures of P-waves depend on only five parameter combinations. As shown by Grechka and Tsvankin (1999), P-wave reflection traveltimes and the operators for dip-moveout (DMO) correction and time migration in homogeneous orthorhombic media are controlled by the NMO velocities from horizontal reflectors in the vertical symmetry planes, $V_{nmo}^{(1)}$ and $V_{nmo}^{(2)}$, and three anellipticity coefficients defined as follows:

$$\eta^{(1)} \equiv \frac{\epsilon^{(1)} - \delta^{(1)}}{1 + 2\delta^{(1)}} \approx \epsilon^{(1)} - \delta^{(1)}, \quad (7)$$

$$\eta^{(2)} \equiv \frac{\epsilon^{(2)} - \delta^{(2)}}{1 + 2\delta^{(2)}} \approx \epsilon^{(2)} - \delta^{(2)}, \quad (8)$$

$$\eta^{(3)} \equiv \frac{\epsilon^{(1)} - \epsilon^{(2)} - \delta^{(3)}[1 + 2\epsilon^{(2)}]}{[1 + 2\epsilon^{(2)}][1 + 2\delta^{(3)}]} \approx \epsilon^{(1)} - \epsilon^{(2)} - \delta^{(3)}. \quad (9)$$

The long-spread reflection traveltimes for orthorhombic media can be described by the general Tsvankin-Thomsen (1994) nonhyperbolic moveout equation with azimuthally varying coefficients:

$$T^2(x, \alpha) = A_0 + A_2(\alpha)x^2 + \frac{A_4(\alpha)x^4}{1 + A(\alpha)x^2}, \quad (10)$$

where

$$A_0 = T_0^2, \quad A_2 = \left. \frac{d(T^2)}{d(x^2)} \right|_{x=0}, \quad \text{and}$$

$$A_4 = \frac{1}{2} \left. \frac{d}{d(x^2)} \left[\frac{d(T^2)}{d(x^2)} \right] \right|_{x=0}.$$

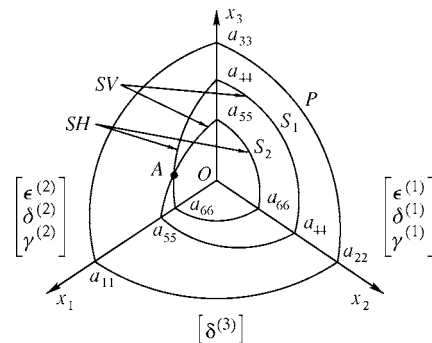


Figure 2. Sketch of body-wave phase-velocity surfaces in orthorhombic media (after Grechka et al., 1999). Tsvankin's (1997) parameters are defined in the mutually orthogonal symmetry planes, which coincide with the coordinate planes. The letter A marks a point (conical) singularity where the phase velocities of the two S-waves are equal to each other.

Here, T_0 is the zero-offset traveltime, A_2 is related to the NMO velocity as $A_2 = V_{\text{nmo}}^{-2}$, and A_4 is the quartic coefficient responsible for nonhyperbolic moveout. The parameter A in the denominator depends on the horizontal group velocity V_{hor} and is designed to make $T(x)$ convergent at large offsets $x \rightarrow \infty$ (Tsvankin and Thomsen, 1994):

$$A = \frac{A_4}{V_{\text{hor}}^{-2} - V_{\text{nmo}}^{-2}}. \quad (11)$$

The hyperbolic coefficient A_2 in equation 10 can be obtained from the results of Grechka and Tsvankin (1999), who use the fact that the azimuthal variation of NMO velocity typically has a simple elliptical form even in arbitrarily anisotropic, heterogeneous media. For a horizontal orthorhombic layer in which the vertical symmetry planes coincide with the coordinate planes $[x_1, x_3]$ and $[x_2, x_3]$, the axes of the NMO ellipse are aligned with the x_1 - and x_2 -directions, which yields (for P-waves)

$$A_2(\alpha) = A_2^{(1)} \sin^2 \alpha + A_2^{(2)} \cos^2 \alpha, \quad (12)$$

$$A_2^{(1)} = \frac{1}{(V_{\text{nmo}}^{(1)})^2} = \frac{1}{V_{P0}^2(1 + 2\delta^{(1)})}, \quad (13)$$

$$A_2^{(2)} = \frac{1}{(V_{\text{nmo}}^{(2)})^2} = \frac{1}{V_{P0}^2(1 + 2\delta^{(2)})}. \quad (14)$$

The azimuth α is computed with respect to the x_1 -axis.

The azimuthally dependent P-wave quartic moveout coefficient A_4 in a horizontal orthorhombic layer has the form (Al-Dajani et al., 1998)

$$A_4(\alpha) = A_4^{(1)} \sin^4 \alpha + A_4^{(2)} \cos^4 \alpha + A_4^{(x)} \sin^2 \alpha \cos^2 \alpha, \quad (15)$$

$$A_4^{(1)} = \frac{-2\eta^{(1)}}{T_0^2 (V_{\text{nmo}}^{(1)})^4}, \quad (16)$$

$$A_4^{(2)} = \frac{-2\eta^{(2)}}{T_0^2 (V_{\text{nmo}}^{(2)})^4}, \quad (17)$$

$$A_4^{(x)} = \frac{2}{T_0^2 (V_{\text{nmo}}^{(1)})^2 (V_{\text{nmo}}^{(2)})^2} \times \left[1 - \sqrt{\frac{(1 + 2\eta^{(1)})(1 + 2\eta^{(2)})}{1 + 2\eta^{(3)}}} \right]. \quad (18)$$

Here, $A_4^{(1)}$ and $A_4^{(2)}$ are the symmetry-plane coefficients and $A_4^{(x)}$ is a cross-term that contributes in off-symmetry directions. Al-Dajani et al. (1998) approximate V_{hor} in equation 11 by the horizontal phase velocity and demonstrate that equation 10 with the moveout coefficients given by equations 11, 12, and 15 is sufficiently accurate for P-wave moveout in models with substantial azimuthal anisotropy. The algorithm of Al-Dajani et al. (1998) based on equation 10 is used below in the numerical modeling of the geometrical spreading in an orthorhombic layer.

A simplified version of equation 10 can be obtained by exploring the approximate kinematic equivalence between the vertical planes of orthorhombic and VTI media. In the

limit of weak anisotropy, out-of-plane phenomena in a horizontal orthorhombic layer have no influence on kinematic signatures, including reflection traveltimes (Tsvankin, 2001, 164). Also, the P-wave phase velocity in any vertical plane of weakly anisotropic orthorhombic media can be described by Thomsen's (1986) VTI equation with azimuthally dependent coefficients ϵ and δ [Tsvankin (2001), equation 1.107]. Therefore, P-wave reflection moveout in a horizontal orthorhombic layer can be approximated by the VTI equation of Alkhalifah and Tsvankin (1995) with the appropriate parameters V_{nmo} and η for each azimuth:

$$T^2(x, \alpha) = T_0^2 + \frac{x^2}{V_{\text{nmo}}^2(\alpha)} - \frac{2\eta(\alpha)x^4}{V_{\text{nmo}}^2(\alpha)\{T_0^2 V_{\text{nmo}}^2(\alpha) + [1 + 2\eta(\alpha)]x^2\}}. \quad (19)$$

The value $V_{\text{nmo}}(\alpha)$ in equation 19 is determined from equations 12–14,

$$V_{\text{nmo}}^2(\alpha) = A_2^{-1} = \frac{(V_{\text{nmo}}^{(1)})^2 (V_{\text{nmo}}^{(2)})^2}{(V_{\text{nmo}}^{(1)})^2 \cos^2 \alpha + (V_{\text{nmo}}^{(2)})^2 \sin^2 \alpha}, \quad (20)$$

and the linearized azimuthally dependent parameter η is given by (Pech and Tsvankin, 2004)

$$\eta(\alpha) = \eta^{(1)} \sin^2 \alpha - \eta^{(3)} \sin^2 \alpha \cos^2 \alpha + \eta^{(2)} \cos^2 \alpha. \quad (21)$$

The nonhyperbolic term in equation 19 can be derived from equation 10 by using the VTI relationships

$$A_4(\alpha) = -\frac{2\eta(\alpha)}{T_0^2 V_{\text{nmo}}^4(\alpha)}, \quad A(\alpha) = \frac{1 + 2\eta(\alpha)}{T_0^2 V_{\text{nmo}}^2(\alpha)}. \quad (22)$$

Although the linearization in the anisotropic parameters implied by the weak-anisotropy approximation formally requires dropping the coefficient $\eta(\alpha)$ from the denominator of equation 19, the complete denominator of the original VTI equation can be retained to increase the accuracy at large source-receiver offsets. Here, equation 19 is used only to obtain analytic expressions for the geometrical spreading in the weak-anisotropy approximation.

Geometrical spreading as a function of moveout coefficients

The derivatives of the traveltime with respect to offset and azimuth needed to obtain the geometrical spreading $L(x, \alpha)$ from equation 5 can be found using the nonhyperbolic moveout equation 10. Explicit expressions for the traveltime derivatives in terms of the azimuthally dependent parameters $A_2(\alpha)$, $A_4(\alpha)$, and $A(\alpha)$ are given in Appendix B. Substituting equations 11, 12, and 15 yields $L(x, \alpha)$ as a function of the medium parameters and the group angle. The group angle ϕ for a single orthorhombic layer can be found in a straightforward way from the reflector depth ($T_0 V_{P0}/2$) and offset x , $\cos \phi = T_0 V_{P0} / \sqrt{x^2 + T_0^2 V_{P0}^2}$.

While the derived equation is well suited for numerical modeling, it does not provide insight into the dependence of

geometrical spreading on the anisotropic parameters. Therefore, we next apply the weak-anisotropy approximation based on the generalized VTI equation 19. The traveltime derivatives in equation 5 are obtained from equation 19 and then linearized in the anellipticity parameters $\eta^{(1,2,3)}$. Further linearization of equation 5 yields the weak-anisotropy approximation for the geometrical spreading discussed below.

Analysis of the weak-anisotropy approximation

Geometrical spreading in the symmetry planes

While the full linearized expression for geometrical spreading is still rather long, it takes a much more concise form in the vertical symmetry planes. For the symmetry plane $[x_1, x_3]$, we find the inverse relative spreading as

$$L^{-1}(x) = \cos^{-1} \phi \frac{A + Bx^2 + Cx^4}{V_{\text{nm0}}^{(1)} V_{\text{nm0}}^{(2)} [T_0^2 (V_{\text{nm0}}^{(2)})^2 + x^2]^3}, \quad (23)$$

where

$$\cos \phi = \frac{T_0 V_{P0}}{\sqrt{x^2 + T_0^2 V_{P0}^2}}, \quad (24)$$

$$A = T_0^5 (V_{\text{nm0}}^{(2)})^6, \quad (25)$$

$$B = T_0^3 (V_{\text{nm0}}^{(2)})^2 [2(1 - 4\eta^{(2)}) (V_{\text{nm0}}^{(2)})^2 + (\eta^{(2)} + \eta^{(3)} - \eta^{(1)}) (V_{\text{nm0}}^{(1)})^2], \quad (26)$$

$$C = T_0 [(1 + \eta^{(2)}) (V_{\text{nm0}}^{(2)})^2 + (\eta^{(2)} + \eta^{(3)} - \eta^{(1)}) (V_{\text{nm0}}^{(1)})^2]. \quad (27)$$

At zero offset, the factor L^{-1} becomes $1/(T_0 V_{\text{nm0}}^{(1)} V_{\text{nm0}}^{(2)})$, which is an exact expression that can be obtained directly from the wavefront curvatures for any strength of anisotropy. As follows from equations 13 and 14 for the NMO velocities, geometrical spreading at vertical incidence is governed by two anisotropic coefficients: $\delta^{(1)}$ and $\delta^{(2)}$. For VTI media, $V_{\text{nm0}}^{(1)} = V_{\text{nm0}}^{(2)}$, and L^{-1} at zero offset reduces to $1/(T_0 V_{\text{nm0}}^2)$; this result is obtained by Tsvankin (1995) and Ursin and Hokstad (2003). If the medium is isotropic, L^{-1} further simplifies to the familiar expression $1/(T_0 V_{P0}^2)$ (Newman, 1973).

The factors B and C in equation 23 can be called the near-offset and far-offset spreading coefficients, respectively. Note that B and C include terms dependent on both in-plane and out-of-plane traveltime (and, therefore, velocity) variations. The P-wave reflection traveltime in the incidence plane is controlled just by the NMO velocity $V_{\text{nm0}}^{(2)}$ and the anisotropic parameter $\eta^{(2)}$ (Grechka and Tsvankin, 1999; Tsvankin, 2001). Hence, the term $(1 - 4\eta^{(2)}) (V_{\text{nm0}}^{(2)})^2$ in the coefficient B represents the in-plane contribution, which coincides with the corresponding (near-offset) spreading factor for VTI media. The other term in the expression for B , $[(\eta^{(2)} + \eta^{(3)} - \eta^{(1)}) (V_{\text{nm0}}^{(1)})^2]$, is entirely the result of azimuthal anisotropy (i.e., a nonzero value of the second traveltime derivative with respect to α). This term vanishes in VTI media where $\eta^{(3)} = 0$ and $\eta^{(1)} = \eta^{(2)}$. Similarly, the far-offset coefficient C contains the

in-plane term $[(1 + \eta^{(2)}) (V_{\text{nm0}}^{(2)})^2]$ and exactly the same out-of-plane term as that in the expression for B .

The inverse spreading L^{-1} in the symmetry plane $[x_2, x_3]$ can be obtained from equations 23–27 by switching the superscripts (1) and (2) in the NMO velocities and the coefficients η . A more detailed comparison of geometrical spreading in the symmetry planes of orthorhombic media with that in VTI media can be found in the numerical example in the next section.

Azimuthal variation of geometrical spreading

Since azimuthal AVO analysis often operates with prestack amplitudes measured at a fixed offset, here we analyze the azimuthally varying spreading factor $L^{-1}(\alpha, x)$ when x is a constant. Using equations 13 and 14 for the symmetry-plane NMO velocities and linearizing both the x^2 and x^4 terms in equation 19 in the anisotropic parameters yields

$$T^2(x, \alpha) = T_0^2 + x^2 \frac{1 - \delta^{(1)} - \delta^{(2)} + (\delta^{(2)} - \delta^{(1)}) \cos 2\alpha}{V_{P0}^2} - 2x^4 \frac{\eta^{(2)} \cos^2 \alpha + \eta^{(1)} \sin^2 \alpha - \eta^{(3)} \cos^2 \alpha \sin^2 \alpha}{T_0^2 V_{P0}^4 (1 + x^2/T_0^2 V_{P0}^2)}. \quad (28)$$

Substituting moveout equation 28 into equation 5 and carrying out further linearization in the anisotropic parameters, we obtain the inverse geometrical spreading as

$$L^{-1}(x, \alpha) = D(x) + E(\alpha) \left[\frac{x}{T_0 V_{P0}} \right]^2 + F(\alpha) \left[\frac{x}{T_0 V_{P0}} \right]^4 + \dots \quad (29)$$

Here, $D(x)$ is an azimuthally independent term that would coincide with L^{-1} in VTI media (the model becomes VTI if the anisotropic coefficients in the vertical symmetry planes are identical and $\eta^{(3)} = 0$). The azimuthally varying terms in equation 29 are expanded in x^2 , and powers of x higher than four are neglected. The coefficients E and F are given by

$$E(\alpha) = \frac{V_{P0}^3 T_0^4}{(V_{P0}^2 T_0^2 + x^2)^{5/2}} [3(\eta^{(1)} - \eta^{(2)}) - (\delta^{(1)} - \delta^{(2)})] \cos 2\alpha; \quad (30)$$

$$F(\alpha) = \frac{V_{P0}^3 T_0^4}{(V_{P0}^2 T_0^2 + x^2)^{5/2}} \left\{ \left[\frac{3}{2} (\delta^{(1)} - \delta^{(2)}) + 9(\eta^{(1)} - \eta^{(2)}) \right] \cos 2\alpha + \frac{9}{8} \eta^{(3)} \cos 4\alpha \right\}. \quad (31)$$

The coefficient $E(\alpha)$ is responsible for the azimuthal dependence of the geometrical spreading at near offsets. Since $E(\alpha)$ is proportional to $\cos 2\alpha$, for small x the function $L^{-1}(\alpha)$ traces out a curve close to an ellipse. In contrast, the far-offset coefficient $F(\alpha)$ contains both $\cos 2\alpha$ and $\cos 4\alpha$, and the form of $L^{-1}(\alpha)$ may substantially deviate from elliptical; this is illustrated by the numerical example in the next section.

The magnitude of the azimuthal variation of geometrical spreading is controlled by the differences $(\delta^{(1)} - \delta^{(2)})$ and $(\eta^{(1)} - \eta^{(2)})$ and, at far offsets, by the coefficient $\eta^{(3)}$. If $\delta^{(1)} = \delta^{(2)}$, $\eta^{(1)} = \eta^{(2)}$, and $\eta^{(3)} = 0$, P-wave velocity becomes azimuthally independent; for purposes of computing P-wave geometrical spreading, the orthorhombic medium becomes equivalent to VTI.

Numerical example

This numerical example illustrates four properties of the inverse spreading L^{-1} in an orthorhombic layer:

- 1) the influence of azimuthal anisotropy on L^{-1} in the vertical symmetry planes,
- 2) the azimuthal variation of L^{-1} at a fixed source-receiver offset,
- 3) the spatial variation of L^{-1} expressed as a function of offset and azimuth, and

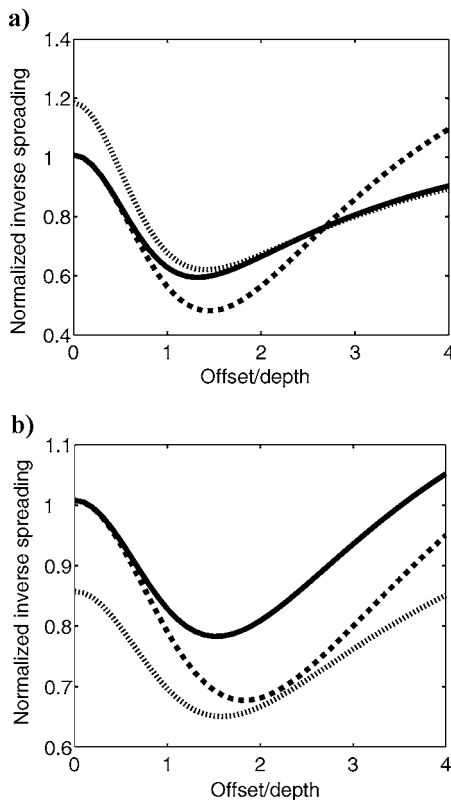


Figure 3. Normalized inverse spreading L^{-1} as a function of the offset-to-depth ratio in the symmetry planes (a) $[x_1, x_3]$ and (b) $[x_2, x_3]$ of a horizontal orthorhombic layer. The solid line is computed using equations 5 and 10, the dashed line is the weak-anisotropy approximation, and the dotted line is L^{-1} in the reference VTI model. The model parameters are $V_{p0} = 2.437$ km/s, $\epsilon^{(1)} = 0.329$, $\epsilon^{(2)} = 0.258$, $\delta^{(1)} = 0.083$, $\delta^{(2)} = -0.078$, and $\delta^{(3)} = -0.106$. The corresponding P-wave moveout parameters are $V_{\text{nmo}}^{(1)} = 2.632$ km/s, $V_{\text{nmo}}^{(2)} = 2.239$ km/s, $\eta^{(1)} = 0.211$, $\eta^{(2)} = 0.398$, and $\eta^{(3)} = 0.193$. The inverse spreading L^{-1} is normalized by its value in the corresponding isotropic layer with the velocity $V_{p0} = 2.437$ km/s.

- 4) the accuracy of the weak-anisotropy approximation for L^{-1} .

We use an orthorhombic model formed by parallel vertical penny-shaped cracks embedded in a VTI background. The stiffness coefficients for this model are given in Schoenberg and Helbig (1997), and the corresponding anisotropic parameters, listed in the caption of Figure 3, are taken from Tsvankin (1997). Although this model has a substantial azimuthal velocity variation, it is dominated by the VTI component, with both ϵ coefficients close to 0.3.

As before, we assume that the coordinate planes coincide with the symmetry planes of the orthorhombic layer. The inverse spreading L^{-1} is found using the formulation based on equations 5 and 10 without making any further approximations in computing the traveltime derivatives and the spreading factor itself. For comparison, we also calculate the weak-anisotropy approximation for L^{-1} by using the moveout equation 19 and linearizing the spreading in the anisotropic coefficients (see the previous section).

Figure 3 displays the inverse spreading L^{-1} (normalized by L^{-1} in the corresponding isotropic model) in the vertical symmetry planes of the layer. Clearly, the influence of anisotropy leads to significant distortions of geometrical spreading in a wide range of offsets for both symmetry planes. As shown by Tsvankin (1995, 2001) for VTI media, the influence of anisotropy causes the amplitude (e.g., the inverse spreading) to decrease with increasing offset if the difference $\epsilon - \delta$ is positive (i.e., $\eta > 0$). Figure 3 confirms that this conclusion remains valid for the symmetry planes of orthorhombic media with moderate azimuthal anisotropy. Indeed, the η coefficients in both vertical symmetry planes ($\eta^{(1)}$ and $\eta^{(2)}$) are positive, and the normalized factor L^{-1} decreases with offset at near-vertical incidence.

Comparison with the spreading in the reference VTI medium (dotted line, Figure 3) helps to quantify the influence of azimuthal anisotropy in both symmetry planes. It is interesting that azimuthal anisotropy changes the spreading factor even at vertical incidence, where for orthorhombic media $L^{-1} = 1/(T_0 V_{\text{nmo}}^{(1)} V_{\text{nmo}}^{(2)})$, while for VTI media, $L^{-1} = 1/(T_0 V_{\text{nmo}}^2)$. For example, if we substitute the NMO velocity in the $[x_1, x_3]$ symmetry plane into the VTI expression, we get a value that is 18% larger than the actual L^{-1} (Figure 3a).

As follows from the weak-anisotropy approximation discussed in the previous section, the influence of azimuthal velocity variations on the offset-dependent part of L^{-1} in the $[x_1, x_3]$ symmetry plane is controlled by the combination $(\eta^{(2)} - \eta^{(1)} + \eta^{(3)})$ of the anellipticity coefficients. Since for our model this combination is positive and relatively large (0.38), L^{-1} in the $[x_1, x_3]$ plane initially decreases with offset slower than in the corresponding VTI medium (Figure 3a). For offset-to-depth ratios exceeding two, however, the factor L^{-1} almost coincides with the VTI value, which contradicts the weak-anisotropy result. Overall, the influence of azimuthal anisotropy is so significant that it is not acceptable to apply 2D amplitude analysis even in the symmetry planes of azimuthally anisotropic media.

Similarly, the factor L^{-1} in the $[x_2, x_3]$ symmetry plane contains the out-of-plane term proportional to $(\eta^{(1)} - \eta^{(2)} + \eta^{(3)})$. For the model at hand, however, this term is close to zero

(0.006), and the offset dependence of the geometrical spreading in the $[x_2, x_3]$ plane is close to that in the reference VTI medium (Figure 3b).

Figure 3 also helps to evaluate the accuracy of the weak-anisotropy approximation for a model that can be characterized as moderately to strongly anisotropic in terms of the magnitude of P-wave velocity variations. While the weak-anisotropy solution is exact at $x = 0$ (because we did not linearize the NMO velocities in the denominator of L^{-1}), it rapidly deviates from the exact factor L^{-1} with increasing offset. Still, the approximation correctly predicts the general character of the function $L^{-1}(x)$ and remains accurate for offset-to-depth ratios of up to about one.

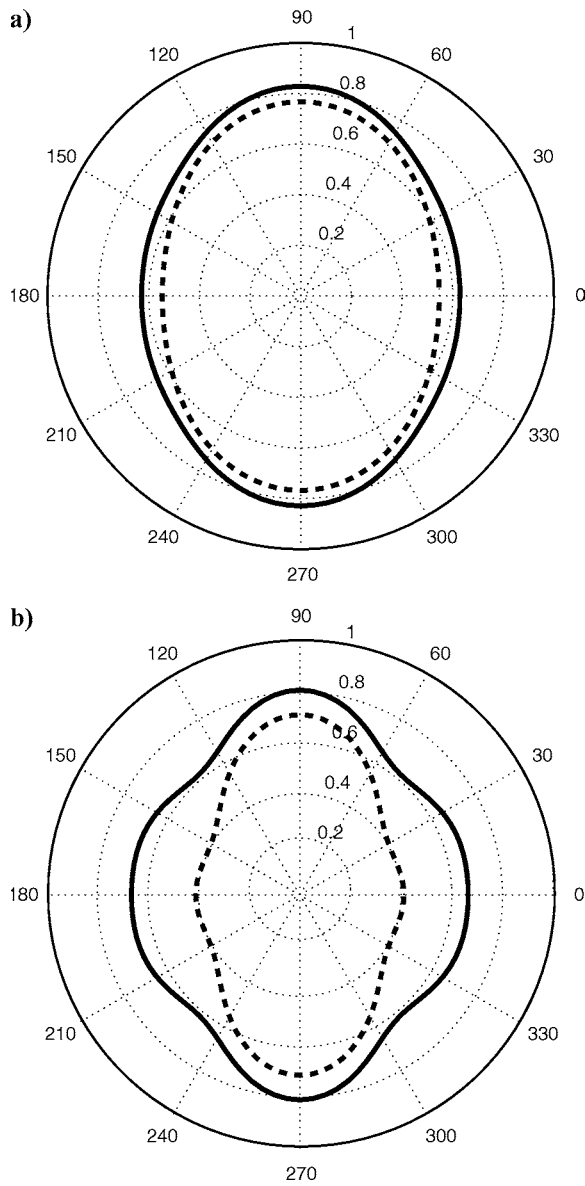


Figure 4. Azimuthal variation of the normalized spreading L^{-1} for the model from Figure 3; the offset-to-depth ratio is equal to (a) one and (b) two. The azimuth α (numbers on the perimeter) is measured with respect to the x_1 -axis. The solid line is computed using equations 5 and 10; the dashed line is the weak-anisotropy approximation.

The azimuthal variation of the normalized spreading L^{-1} at two different offsets is plotted in Figure 4. Since the geometrical spreading in our model is symmetric with respect to both vertical coordinate planes, the signature of L^{-1} is repeated in each quadrant. For the offset equal to the reflector depth, the azimuthal variation of L^{-1} is close to elliptical, as predicted by the weak-anisotropy approximation (Figure 4a). The fractional difference between the values of L^{-1} in the symmetry planes, which determines the overall magnitude of the azimuthal variation of the inverse geometrical spreading, is about 30%. Hence, for this model the eccentricity of the geometrical-spreading ellipse exceeds that of the NMO ellipse (18%). For larger offset-to-depth ratios, the shape of the curve $L^{-1}(\alpha)$ becomes more complicated and, in agreement with the weak-anisotropy approximation 31 for the x^4 term, deviates from an ellipse (Figure 4).

A complete picture of the spatial variations of the spreading factor in our model is given in Figure 5a, where L^{-1} is computed as a function of both offset and azimuth. The combined influence of polar and azimuthal anisotropy creates a rather complicated pattern of the normalized factor L^{-1} , with

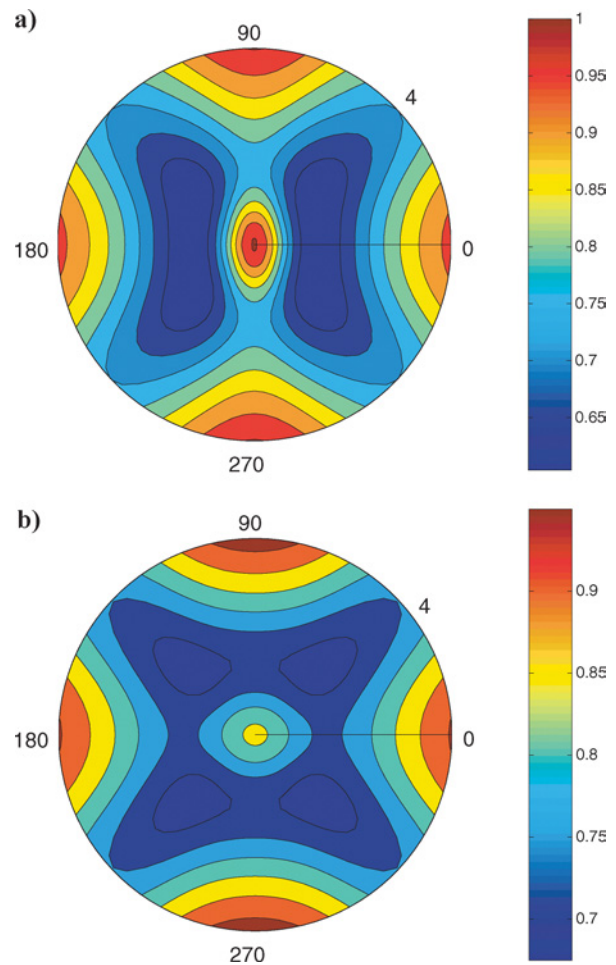


Figure 5. Map of the normalized inverse spreading L^{-1} as a function of offset and azimuth. (a) Computed for the model from Figure 3; (b) the sign of the parameter $\delta^{(2)}$ is changed from negative to positive (i.e., $\delta^{(2)} = 0.078$). The offset-to-depth ratio varies from zero to four.

Table 1. Parameters of a four-layer model that includes two orthorhombic layers (layers 2 and 3) with aligned vertical symmetry planes.

Layer	Symmetry type	V_{P0} (km/s)	Thickness (km)	$\epsilon^{(1)}$	$\epsilon^{(2)}$	$\delta^{(1)}$	$\delta^{(2)}$	$\delta^{(3)}$
1	Isotropic	1.5	0.2	0	0	0	0	0
2	Orthorhombic	2.437	0.9	0.329	0.258	0.083	-0.078	-0.106
3	Orthorhombic	3.0	0.9	0.25	0.15	0.05	-0.1	0.15
4	Isotropic	3.2	0.5	0	0	0	0	0

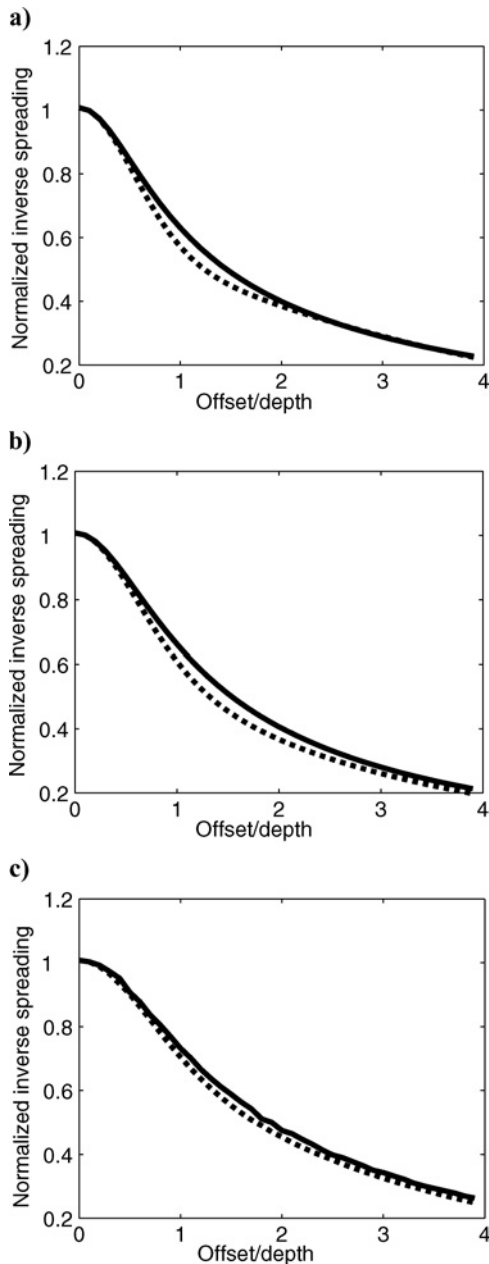


Figure 6. Comparison of the inverse relative spreading computed by our method (dashed line) and ANRAY (solid) for the model from Figure 3. The source-receiver line is oriented (a) along the x_1 -axis, (b) at 45° with the x_1 -axis, and (c) along the x_2 -axis.

substantial azimuthal variations and pronounced deviations from the corresponding isotropic values. The largest anisotropy-induced distortions of the geometrical spreading, reaching 40%, are observed near the $[x_1, x_3]$ plane for offset-to-depth ratios of about 1.5.

The significant azimuthal variation of L^{-1} at near offsets is partly caused by the opposite signs of the δ coefficients in the vertical symmetry planes. In Figure 5b, we change the sign of $\delta^{(2)}$ (the other model parameters remain the same), which reduces the differences between the symmetry-plane NMO velocities ($V_{\text{nmo}}^{(1)}$ and $V_{\text{nmo}}^{(2)}$) and between the corresponding η coefficients ($\eta^{(1)}$ and $\eta^{(2)}$). Although the geometrical spreading becomes much less dependent on azimuth at near offsets, the azimuthal variation of L^{-1} at moderate and far offsets in Figure 5b is still quite pronounced.

COMPARISON WITH DYNAMIC RAY TRACING

To verify the accuracy of our algorithm (equation 4) based on the nonhyperbolic moveout equation 10, we compared our results with the spreading computed by the dynamic ray-tracing code ANRAY (Gajewski and Pšenčík, 1990). The comparison was carried out for a single orthorhombic layer with the parameters of the Schoenberg-Helbig model used previously and a more complicated medium composed of two orthorhombic and two isotropic layers (Table 1). To facilitate the conversion from the relative spreading produced by our algorithm to the absolute spreading computed by ANRAY, we placed a thin, 10-m isotropic layer on top of the 1000-m-thick orthorhombic layer. The moveout coefficients were found by fitting equation 10 to ray-traced traveltimes using the least-squares method. The group angle for the layered model was estimated from the slope of the traveltimes curve and the velocity in the subsurface isotropic layer.

For both models, the geometrical spreading calculated by our method is close to the results of dynamic ray tracing for a wide range of offsets (Figures 6 and 7). Small deviations from the ray-traced values can be explained by the approximate nature of the Tsvankin-Thomsen nonhyperbolic moveout equation and, possibly, by numerical errors in ANRAY. Since equation 4 includes second-order traveltimes derivatives, the spreading computed by our algorithm is sensitive to relatively small correlated errors in the moveout function.

Still, Figure 7 demonstrates that equation 10 adequately describes P-wave moveout, not just for a single layer but also for a stack of azimuthally anisotropic layers with aligned vertical symmetry planes. For layered media, all moveout coefficients become effective values that depend on the interval NMO velocities and η parameters.

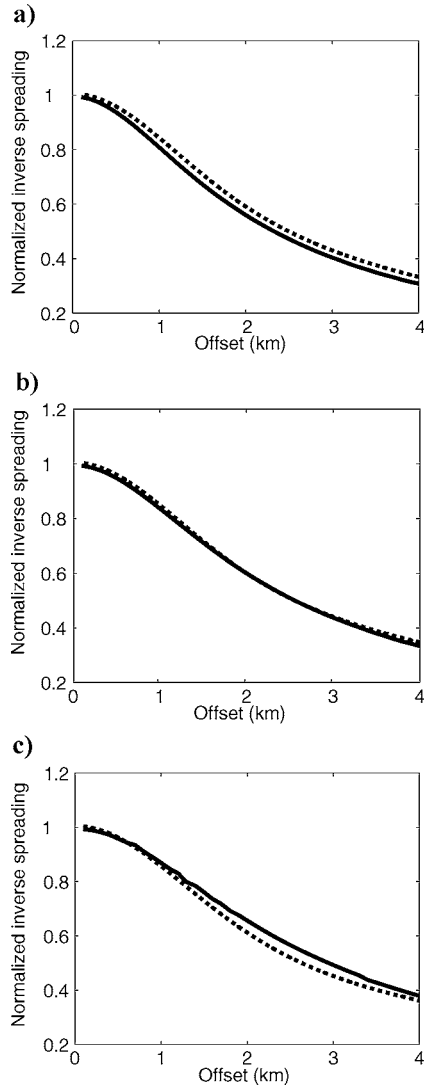


Figure 7. Comparison of the inverse relative spreading computed by our method (dashed line) and ANRAY (solid) for the layered orthorhombic model from Table 1. (We used the reflection from the bottom of the third layer.) The source-receiver line is oriented (a) along the x_1 -axis, (b) at 45° with the x_1 -axis, and (c) along the x_2 -axis.

DISCUSSION AND CONCLUSIONS

Although geometrical spreading of reflected waves is determined by the medium properties around the whole raypath, it can be obtained from the reflection traveltime and the group angles at the source and receiver locations. Using ray theory, we showed that for pure (unconverted) modes recorded above a horizontally layered medium, relative geometrical spreading can be expressed as a simple function of the traveltime derivatives with respect to offset and azimuth and the group angles at the surface. Although this equation does not account for lateral heterogeneity, it involves no restrictions on the number of layers above the reflector or the type of symmetry in each layer.

To describe the geometrical spreading of P-waves in orthorhombic media, we combined our general result with the Tsvankin-Thomsen nonhyperbolic moveout equation for a homogeneous, horizontal orthorhombic layer. The P-wave reflection traveltime and, therefore, the geometrical spreading for this model are governed by the NMO velocities $V_{\text{nmo}}^{(1)}$ and $V_{\text{nmo}}^{(2)}$ in the vertical symmetry planes and the anellipticity coefficients $\eta^{(1)}$, $\eta^{(2)}$, and $\eta^{(3)}$. To explain the dependence of inverse spreading L^{-1} on these parameters, we used the weak-anisotropy approximation based on linearization in the anisotropic coefficients. The analytic results were verified by numerical tests for an orthorhombic model formed by vertical penny-shaped cracks embedded in a VTI matrix.

Although the geometrical-spreading signature in an orthorhombic layer is repeated in each quadrant, the variation of the factor L^{-1} with offset and azimuth has a rather complicated character. For the model used here, the error of the isotropic equation for geometrical spreading reaches a maximum of 40% in the intermediate offset range (i.e., for the offset-to-depth ratio between one and two). The azimuthal variation $L^{-1}(\alpha)$ for a fixed offset is close to elliptical at relatively small offset-to-depth ratios of up to one. For larger offsets, $L^{-1}(\alpha)$ deviates from an ellipse and may have intermediate minima or maxima between the symmetry planes.

Both analytical and numerical results show that the spreading factor L^{-1} is substantially influenced by azimuthal velocity variations even in the vertical symmetry planes. At zero offset (vertical incidence), exact inverse geometrical spreading is given by a simple equation that involves only the NMO velocities in both symmetry planes: $L^{-1} = 1/(T_0 V_{\text{nmo}}^{(1)} V_{\text{nmo}}^{(2)})$. The offset-dependent part of L^{-1} in the symmetry planes can be separated (in the weak-anisotropy approximation) into the in-plane term, identical to the factor L^{-1} in the corresponding VTI medium, and the out-of-plane term associated with azimuthal anisotropy. In the $[x_1, x_3]$ plane, the contribution of azimuthal velocity variation is proportional to the combination $(\eta^{(2)} - \eta^{(1)} + \eta^{(3)})$, and in the $[x_2, x_3]$ plane it is proportional to $(\eta^{(1)} - \eta^{(2)} + \eta^{(3)})$.

The large magnitude of the anisotropy-induced distortions of the factor L^{-1} means that reliable interpretation of the wide-azimuth AVO response for media with azimuthally anisotropic overburden is impossible without properly correcting for geometrical spreading. The estimation and removal of geometrical spreading can be accomplished by applying equation 4 with the best-fit traveltime function. Analytic representations of reflection moveout can facilitate the spreading correction by providing a smooth, accurate approximation for the measured traveltimes.

In practice, however, complications may arise from the high sensitivity of the geometrical spreading to lateral heterogeneity, small errors in the best-fit traveltimes, or distortions in the group (ray) angles. For example, it is difficult to estimate the group angles at the source and receiver locations using just the acquisition geometry and traveltime data unless the subsurface layer is isotropic. Even for the homogeneous orthorhombic model studied here, the group angle $\phi^s = \phi^r$ can be found in a straightforward way only if the layer thickness is known. Practical issues involved in the geometrical-spreading correction for layered azimuthally anisotropic media are yet to be investigated.

ACKNOWLEDGMENTS

We are grateful to Vladimir Grechka (Shell), Ivan Pšenčík (Czech Academy of Sciences), and Bjorn Ursin (Norwegian University of Science and Technology) for useful discussions and their help with ray-tracing codes. The reviews by Vladimir Grechka, Matt Haney (CSM), Ketil Hokstad (Statoil), Ken Lerner (CSM), Ivan Pšenčík, and Claudia Vanelle helped to improve the manuscript substantially. We thank Debashish Sarkar (CSM, now at GX Technology) for valuable technical assistance with this project. The support for this work was provided by the Consortium Project on Seismic Inverse Methods for Complex Structures at the Center for Wave Phenomena, Colorado School of Mines, and by the Chemical Sciences, Geosciences and Biosciences Division, Office of Basic Energy Sciences, U.S. Department of Energy.

APPENDIX A

RELATIVE GEOMETRICAL SPREADING AS A FUNCTION OF REFLECTION TRAVELTIME

As discussed in the main text, the relative geometrical spreading $L(R, S)$ can be obtained in terms of the mixed second-order traveltimes derivatives with respect to the source and receiver coordinates using equations 2 and 3. Here, we express $L(R, S)$ through the multiazimuth reflection traveltimes of a pure (unconverted) mode recorded over a laterally homogeneous medium.

The spreading factor $L(R, S)$ can be found from the traveltimes-derivative matrix \mathbf{M}^{mix} given in equation 3:

$$\mathbf{M}^{\text{mix}} = \begin{bmatrix} \frac{\partial^2 T(x^r, x^s)}{\partial x_1^s \partial x_1^r} & \frac{\partial^2 T(x^r, x^s)}{\partial x_1^s \partial x_2^r} \\ \frac{\partial^2 T(x^r, x^s)}{\partial x_2^s \partial x_1^r} & \frac{\partial^2 T(x^r, x^s)}{\partial x_2^s \partial x_2^r} \end{bmatrix}, \quad (\text{A-1})$$

where x_1^s and x_2^s are the horizontal Cartesian coordinates of the source and where x_1^r and x_2^r are the coordinates of the receiver. In general, \mathbf{M}^{mix} is a function of four independent variables, $x_1^{s,r}$ and $x_2^{s,r}$. For laterally homogeneous media considered in this paper, however, the number of independent variables of \mathbf{M}^{mix} reduces from four to two. Indeed, in the absence of lateral heterogeneity, the traveltimes T of a pure mode on a horizontal surface depends only on the distance x between the source and the receiver and the azimuth α of the source-receiver line with respect to the x_1 -axis:

$$x = \sqrt{(x_1^r - x_1^s)^2 + (x_2^r - x_2^s)^2}, \quad (\text{A-2})$$

$$\alpha = \tan^{-1} \left[\frac{x_2^r - x_2^s}{x_1^r - x_1^s} \right]. \quad (\text{A-3})$$

If the traveltimes T is expressed as a function of x and α , the elements of the matrix \mathbf{M}^{mix} become

$$\begin{aligned} \frac{\partial^2 T}{\partial x_1^s \partial x_1^r} &= \frac{\partial^2 T}{\partial x^2} \frac{\partial x}{\partial x_1^s} \frac{\partial x}{\partial x_1^r} + \frac{\partial T}{\partial x} \frac{\partial^2 x}{\partial x_1^s \partial x_1^r} + \frac{\partial^2 T}{\partial \alpha^2} \frac{\partial \alpha}{\partial x_1^s} \frac{\partial \alpha}{\partial x_1^r} \\ &+ \frac{\partial T}{\partial \alpha} \frac{\partial^2 \alpha}{\partial x_1^s \partial x_1^r}, \end{aligned} \quad (\text{A-4})$$

$$\begin{aligned} \frac{\partial^2 T}{\partial x_1^s \partial x_2^r} &= \frac{\partial^2 T}{\partial x^2} \frac{\partial x}{\partial x_1^s} \frac{\partial x}{\partial x_2^r} + \frac{\partial T}{\partial x} \frac{\partial^2 x}{\partial x_1^s \partial x_2^r} + \frac{\partial^2 T}{\partial \alpha^2} \frac{\partial \alpha}{\partial x_1^s} \frac{\partial \alpha}{\partial x_2^r} \\ &+ \frac{\partial T}{\partial \alpha} \frac{\partial^2 \alpha}{\partial x_1^s \partial x_2^r}, \end{aligned} \quad (\text{A-5})$$

$$\frac{\partial^2 T}{\partial x_2^s \partial x_1^r} = \frac{\partial^2 T}{\partial x^2} \frac{\partial x}{\partial x_2^s} \frac{\partial x}{\partial x_1^r}, \quad (\text{A-6})$$

$$\begin{aligned} \frac{\partial^2 T}{\partial x_2^s \partial x_2^r} &= \frac{\partial^2 T}{\partial x^2} \frac{\partial x}{\partial x_2^s} \frac{\partial x}{\partial x_2^r} + \frac{\partial T}{\partial x} \frac{\partial^2 x}{\partial x_2^s \partial x_2^r} + \frac{\partial^2 T}{\partial \alpha^2} \frac{\partial \alpha}{\partial x_2^s} \frac{\partial \alpha}{\partial x_2^r} \\ &+ \frac{\partial T}{\partial \alpha} \frac{\partial^2 \alpha}{\partial x_2^s \partial x_2^r}. \end{aligned} \quad (\text{A-7})$$

The derivatives of x and α with respect to the source and receiver coordinates can be obtained from equations A-2 and A-3:

$$\frac{\partial x}{\partial x_i^s} = \frac{x_i^s - x_i^r}{x}, \quad \frac{\partial x}{\partial x_i^r} = \frac{x_i^r - x_i^s}{x} \quad (i = 1, 2), \quad (\text{A-8})$$

$$\frac{\partial \alpha}{\partial x_1^s} = \frac{x_2^r - x_2^s}{x^2}, \quad \frac{\partial \alpha}{\partial x_2^s} = \frac{x_1^s - x_1^r}{x^2}, \quad (\text{A-9})$$

$$\frac{\partial \alpha}{\partial x_1^r} = \frac{x_2^s - x_2^r}{x^2}, \quad \frac{\partial \alpha}{\partial x_2^r} = \frac{x_1^r - x_1^s}{x^2}, \quad (\text{A-10})$$

$$\frac{\partial^2 x}{\partial x_1^s \partial x_1^r} = \frac{-(x_2^r - x_2^s)^2}{x^3}, \quad (\text{A-11})$$

$$\frac{\partial^2 x}{\partial x_1^s \partial x_2^r} = \frac{(x_1^r - x_1^s)(x_2^r - x_2^s)}{x^3}, \quad (\text{A-12})$$

$$\frac{\partial^2 x}{\partial x_2^s \partial x_2^r} = \frac{-(x_1^r - x_1^s)^2}{x^3}, \quad (\text{A-13})$$

$$\frac{\partial^2 \alpha}{\partial x_1^s \partial x_1^r} = \frac{-2(x_1^r - x_1^s)(x_2^r - x_2^s)}{x^4}, \quad (\text{A-14})$$

$$\frac{\partial^2 \alpha}{\partial x_1^s \partial x_2^r} = \frac{(x_1^r - x_1^s)^2 - (x_2^r - x_2^s)^2}{x^4}, \quad (\text{A-15})$$

$$\frac{\partial^2 \alpha}{\partial x_2^s \partial x_2^r} = \frac{2(x_1^r - x_1^s)(x_2^r - x_2^s)}{x^4}. \quad (\text{A-16})$$

Substituting equations A-8 through A-16 into equations A-4 through A-7 yields

$$\begin{aligned} \frac{\partial^2 T}{\partial x_1^s \partial x_1^r} &= -\frac{\partial^2 T}{\partial x^2} \frac{(x_1^r - x_1^s)^2}{x^2} - \frac{\partial T}{\partial x} \frac{(x_2^r - x_2^s)^2}{x^3} \\ &- \frac{\partial^2 T}{\partial \alpha^2} \frac{(x_2^r - x_2^s)^2}{x^4} - \frac{\partial T}{\partial \alpha} \frac{2(x_1^r - x_1^s)(x_2^r - x_2^s)}{x^4}, \end{aligned} \quad (\text{A-17})$$

$$\begin{aligned} \frac{\partial^2 T}{\partial x_1^s \partial x_2^r} &= \frac{\partial^2 T}{\partial x^2} \frac{-(x_1^r - x_1^s)(x_2^r - x_2^s)}{x^2} \\ &+ \frac{\partial T}{\partial x} \frac{(x_1^r - x_1^s)(x_2^r - x_2^s)}{x^3} \end{aligned} \quad (\text{A-18})$$

$$\begin{aligned} &+ \frac{\partial^2 T}{\partial \alpha^2} \frac{(x_1^r - x_1^s)(x_2^r - x_2^s)}{x^4} \\ &+ \frac{\partial T}{\partial \alpha} \frac{(x_1^r - x_1^s)^2 - (x_2^r - x_2^s)^2}{x^4}, \end{aligned} \quad (\text{A-19})$$

$$\frac{\partial^2 T}{\partial x_2^s \partial x_2^r} = -\frac{\partial^2 T}{\partial x^2} \frac{(x_2^r - x_2^s)^2}{x^2} - \frac{\partial T}{\partial x} \frac{(x_1^r - x_1^s)^2}{x^3} - \frac{\partial^2 T}{\partial \alpha^2} \frac{(x_1^r - x_1^s)^2}{x^4} + \frac{\partial T}{\partial \alpha} \frac{2(x_1^r - x_1^s)(x_2^r - x_2^s)}{x^4}. \quad (\text{A-20})$$

The determinant of the matrix \mathbf{M}^{mix} is then found as

$$\det \mathbf{M}^{\text{mix}} = \frac{\partial^2 T}{\partial x^2} \frac{\partial T}{\partial x} \frac{1}{x} + \frac{\partial^2 T}{\partial x^2} \frac{\partial^2 T}{\partial \alpha^2} \frac{1}{x^2} - \left(\frac{\partial T}{\partial \alpha} \right)^2 \frac{1}{x^4}. \quad (\text{A-21})$$

Finally, using equation A-21, the relative geometrical spreading (equation 2) can be expressed through the travel-time derivatives with respect to the offset x and azimuth α :

$$L(R, S) = L(x, \alpha) = (\cos \phi^s \cos \phi^r)^{1/2} \left[\frac{\partial^2 T}{\partial x^2} \frac{\partial T}{\partial x} \frac{1}{x} + \frac{\partial^2 T}{\partial x^2} \frac{\partial^2 T}{\partial \alpha^2} \frac{1}{x^2} - \left(\frac{\partial T}{\partial \alpha} \right)^2 \frac{1}{x^4} \right]^{-1/2}. \quad (\text{A-22})$$

APPENDIX B

TRAVELTIME DERIVATIVES FROM THE NONHYPERBOLIC MOVEOUT EQUATION

The P-wave nonhyperbolic (long-spread) reflection travel-time can be described by the Tsvankin-Thomsen (1994) moveout equation:

$$T^2(x, \alpha) = T_0^2 + A_2(\alpha)x^2 + \frac{A_4(\alpha)x^4}{1 + A(\alpha)x^2}, \quad (\text{B-1})$$

where the moveout coefficients A_2 , A_4 , and A generally vary with the azimuth α .

The derivatives of the traveltime with respect to the offset x are given by

$$\frac{\partial T}{\partial x} = \frac{1}{T} \left[A_2 x + \frac{2A_4 x^3}{1 + Ax^2} - \frac{AA_4 x^5}{(1 + Ax^2)^2} \right] \quad (\text{B-2})$$

and

$$\frac{\partial^2 T}{\partial x^2} = \frac{1}{T} \left[f(x) - \left(\frac{\partial T}{\partial x} \right)^2 \right]; \quad (\text{B-3})$$

$$f(x) \equiv A_2 + \frac{6A_4 x^2}{1 + Ax^2} - \frac{9AA_4 x^4}{(1 + Ax^2)^2} + \frac{4A_4 A^2 x^6}{(1 + Ax^2)^3}. \quad (\text{B-4})$$

Differentiating equation B-1 with respect to azimuth yields

$$\frac{\partial T}{\partial \alpha} = \frac{1}{2T} \left[A_2' x^2 + \frac{A_4' x^4}{1 + Ax^2} - \frac{A_4 A' x^6}{(1 + Ax^2)^2} \right] \quad (\text{B-5})$$

and

$$\begin{aligned} \frac{\partial^2 T}{\partial \alpha^2} = & \frac{\partial T}{\partial \alpha} \frac{1}{2T^2} \left[A_2' x^2 + \frac{A_4' x^4}{1 + Ax^2} - \frac{A_4 A' x^6}{(1 + Ax^2)^2} \right] \\ & + \frac{1}{2T} \left[A_2'' x^2 + \frac{A_4'' x^4}{1 + Ax^2} - \frac{A_4 A'' x^6}{(1 + Ax^2)^2} \right. \\ & \left. - \frac{2A' A_4' x^6}{(1 + Ax^2)^2} + \frac{2A_4 (A')^2 x^8}{(1 + Ax^2)^3} \right]. \quad (\text{B-6}) \end{aligned}$$

Here, A_2' , A_4' , A' , A_2'' , A_4'' , and A'' are the first and second derivatives of the moveout coefficients with respect to α . For the model of a single orthorhombic layer, these derivatives can be found from the explicit expressions for A_2 , A_4 , and A given in the main text.

REFERENCES

- Al-Dajani, A., I. Tsvankin, and M. N. Toksöz, 1998, Nonhyperbolic reflection moveout for azimuthally anisotropic media: 68th Annual International Meeting, SEG, Expanded Abstracts, 1479–1482.
- Alkhalifah, T., and I. Tsvankin, 1995, Velocity analysis for transversely isotropic media: *Geophysics*, **60**, 1550–1566.
- Bakulin, A., V. Grechka, and I. Tsvankin, 2000, Estimation of fracture parameters from reflection seismic data — Part II: Fractured models with orthorhombic symmetry: *Geophysics*, **65**, 1803–1817.
- Červený, V., 2001, *Seismic ray theory*: Cambridge University Press.
- Gajewski, D., and I. Pšenčík, 1990, Vertical seismic profile synthetics by dynamic ray tracing in laterally varying layered anisotropic structure: *Journal of Geophysical Research*, **95**, 11301–11315.
- Goldin, S., 1986, Seismic traveltime inversion: SEG.
- Grechka, V., and I. Tsvankin, 1998, Feasibility of nonhyperbolic moveout inversion in transversely isotropic media: *Geophysics*, **63**, 957–969.
- , 1999, 3-D moveout velocity analysis and parameter estimation for orthorhombic media: *Geophysics*, **64**, 820–837.
- Grechka, V., S. Theophanis, and I. Tsvankin, 1999, Joint inversion of P- and PS-waves in orthorhombic media: Theory and a physical modeling study: *Geophysics*, **64**, 146–161.
- Lynn, H. B., D. Campagna, K. M. Simon, and W. E. Beckham, 1999, Relationship of P-wave seismic attributes, azimuthal anisotropy, and commercial gas pay in 3-D P-wave multi-azimuth data, Rulison field, Piceance basin, Colorado: *Geophysics*, **64**, 1312–1328.
- Mallick, S., K. Craft, and L. Meister, 1998, Determination of the principal directions of azimuthal anisotropy from P-wave seismic data: *Geophysics*, **63**, 692–706.
- Martinez, R. D., 1993, Wave propagation effects on amplitude variation with offset measurements: A modeling study: *Geophysics*, **58**, 534–543.
- Maultzsch, S., S. Horne, S. Archer, and H. Burkhardt, 2003, Effects of an anisotropic overburden on azimuthal amplitude analysis in horizontal transverse isotropic media: *Geophysical Prospecting*, **51**, 61–74.
- Newman, P., 1973, Divergence effects in a layered earth: *Geophysics*, **38**, 481–488.
- Pech, A., and I. Tsvankin, 2004, Quartic moveout coefficient for a dipping azimuthally anisotropic layer: *Geophysics*, **69**, 699–707.
- Rüger, A., 2001, Reflection coefficients and azimuthal AVO analysis in anisotropic media: SEG.
- Rüger, A., and I. Tsvankin, 1997, Using AVO for fracture detection: Analytic basis and practical solutions: *The Leading Edge*, **16**, 1429–1434.
- Schoenberg, M., and K. Helbig, 1997, Orthorhombic media: Modeling elastic wave behavior in a vertically fractured earth: *Geophysics*, **62**, 1954–1974.
- Thomsen, L., 1986, Weak elastic anisotropy: *Geophysics*, **51**, 1954–1966.
- Tsvankin, I., 1995, Body-wave radiation patterns and AVO in transversely isotropic media: *Geophysics*, **60**, 1409–1425.
- , 1997, Anisotropic parameters and P-wave velocity for orthorhombic media: *Geophysics*, **62**, 1292–1309.
- , 2001, Seismic signatures and analysis of reflection data in anisotropic media: Elsevier Science Publishing Co., Inc.
- Tsvankin, I., and L. Thomsen, 1994, Nonhyperbolic reflection moveout in anisotropic media: *Geophysics*, **59**, 1290–1304.
- Ursin, B., and K. Hokstad, 2003, Geometrical spreading in a layered transversely isotropic medium with vertical symmetry axis: *Geophysics*, **68**, 2082–2091.
- Vanelle, C., and D. Gajewski, 2003, Determination of geometrical spreading from traveltimes: *Journal of Applied Geophysics*, **54**, 391–400.